

Time and energy-resolved two photon photoemission of the Cu(1 0 0) and Cu(1 1 1) metal surfaces

Daniele Varsano ^{*}, M.A.L. Marques, Angel Rubio

Departamento de Física de Materiales, Facultad de Químicas, Universidad del País Vasco and Donostia International Physics Center (DIPC), 20080 San Sebastian, Spain

Abstract

We present calculations on energy- and time-resolved two photon photoemission spectra of image states in Cu(1 0 0) and Cu(1 1 1) surfaces. The surface is modeled by a 1D effective potential and the states are propagated within a real-space, real-time method. To obtain the energy-resolved spectra we employ a geometrical approach based on a subdivision of space into two regions. We treat electronic inelastic effects by taking into account the scattering rates calculated within a GW scheme. To get further insight into the decaying mechanism we have also studied the effect of the variation of the classical Hartree potential during the excitation. This effect turns out to be small.

© 2004 Published by Elsevier B.V.

1. Introduction

The presence of a metal surface creates electron states that do not exist in the bulk metal. For example, an electron situated at a distance z from the metal surface experiences an attractive force, $F(z) = -e^2/(2z)^2$, equivalent to that produced by its image charge situated at distance z inside the metal. For large z , the potential generated by this surface induced charge approaches the classical image potential, $V(z) = -e^2/4z$.¹ When the metal

has a surface band gap near the vacuum level, the electrons below the vacuum level are trapped between the well of the image potential and the surface barrier. These quantized states correspond to image potential states, and are spatially localized in the region in front of the surface (see Fig. 1). Metal image states typically have a large spatial extension, but barely penetrate the bulk metal. They form a Rydberg-like series with energies, E_n , approximately given by [1]:

$$E_n = -\frac{0.85}{(n+a)^2} \quad [\text{eV}], \quad (1)$$

where n is a positive integer, and $0 \leq a \leq 0.5$ represents the quantum defect (which depends on the position and width of the gap). The energy of an electron trapped in an image state and moving parallel to the surface with momentum \mathbf{k}_{\parallel} is therefore

^{*} Corresponding author. Tel.: +34-94-3015-389; fax: +34-94-3015-600.

E-mail address: wabvavad@sc.ehu.es (D. Varsano).

¹ This expression corresponds to assuming an infinite repulsive barrier at the surface. In the more general case we have $V(z) = -\frac{e^2}{4(z-z_{\text{im}})} \frac{\epsilon-1}{\epsilon+1}$, where z_{im} is the position of the image plane (that depends on the electronic and structural properties of the surface) and ϵ is the static dielectric constant of the surface.

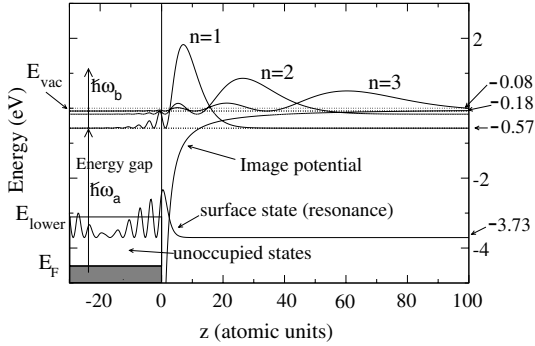


Fig. 1. Schematic picture of a 2PPE experiment for a typical metallic surface with a surface band gap close to the Fermi level. The energy $\hbar\omega_a$ corresponds to the pump photon and $\hbar\omega_b$ to the probe photon in 2PPE. On the right side we show the tail of the image potential, the densities of the surface state and first three image potential states of Cu(100) calculated with the model potential of Ref. [2], and their corresponding binding energies. By E_F , E_{lower} and E_{vac} we denote the Fermi energy, the lower edge of the energy gap and the vacuum energy.

$$E = \frac{\hbar^2 k_{\parallel}^2}{2m_e} + E_n \quad (2)$$

In contrast to bulk states, the small overlap between surface states and bulk states reduces considerably the inelastic electron scattering, leading to a long lifetime, τ_n , of the image states, that scales asymptotically with the quantum number n as $\tau_n \propto n^3$ [2]. Due to this fact, these states are very interesting for the study of electron correlations. Furthermore, image states play an important role in the laser induced chemical control of reactivity at metal surfaces. It is therefore not surprising the considerable number of studies focusing on this subject (see Ref. [3] and references within).

Image potential states of different surfaces have been observed experimentally [4]. A powerful technique to measure their energy and lifetime is two photon photoemission spectroscopy (2PPE) [5]. Recently, and with the advent of ultrafast laser technology it became possible to perform time-resolved 2PPE spectroscopy (TR2PPE), which allowed, with the technique of quantum beat spectroscopy [6,7], the direct measurement of the lifetime of image states, even for states with large

quantum number n . The 2PPE technique is depicted schematically in Fig. 1. One photon (pump), of energy $\hbar\omega_a$, excites an electron from an occupied state below the Fermi energy (E_F) to an image potential state of quantum number n . Then a second photon (probe), with energy $\hbar\omega_b$, ejects the electron out of the surface, above the vacuum energy. This electron has a kinetic energy $E_k = \hbar\omega_b - E_n$, that is measured in a detector far away from the surface. By varying the delay between the pump and probe pulses, the intensity of the 2PPE signal as a function of the delay will reflect the evolution of the population of the state n . From this information it is then possible to extract the lifetime of the state n .

Lifetimes of image states for different metal surfaces have been calculated in the framework of the self-energy formalism in the GW approximation [3,8]. The results obtained happen to be in rather good agreement with experiments. For example, the calculated lifetime of the first three image potential states of the Cu(100) surface are $\tau_1^{\text{theor}} = 30$ fs, $\tau_2^{\text{theor}} = 132$ fs, and $\tau_3^{\text{theor}} = 367$ fs [3], while the experimental values are $\tau_1^{\text{exp}} = 40 \pm 6$ fs, $\tau_2^{\text{exp}} = 110 \pm 10$ fs, and $\tau_3^{\text{exp}} = 300 \pm 15$ fs [6], while for the first image state of Cu(111) surface the theoretical lifetime is $\tau_1^{\text{theor}} = 17.5$ fs [3] and the experimental is $\tau_1^{\text{exp}} = 15 \pm 5$ fs [9].

In the present paper we present calculations on energy-resolved 2PPE spectra of Cu(100) and Cu(111) surfaces. Our theoretical approach is based on the propagation of an electron wavepacket in an one-dimensional model potential [2] simulating the copper surface. The finite electronic lifetimes of the image potential states are taken into account by an empirical self-energy term. The photoemission spectra are obtained through a geometrical scheme described in Ref. [10]. Note that in this approach the potential is fixed during the whole simulations, i.e., the change of the electronic screening during the excitation is not taken into account. This could be important for short laser excitations as done in TR2PPE.

To assert the relevance of this approximation we also performed time-dependent simulations of the copper surface, but including the change of the Hartree potential due to the electronic excitations.

2. Method

To model the copper surface we used a one-dimensional slab of 48 copper layers, surrounded by 290 a.u. of vacuum on each side. The large portion of vacuum is necessary in order to describe the four first image potential wave functions (see Fig. 1). The bulk and image potentials are modeled by the 1D potential model of Ref. [2]. This model reproduces the position and the width of the energy gap, as well as the energy of the surface state and of the first image potential state. Furthermore, it provides a good description of the electronic structure of simple and noble metal surfaces [2]. In this model the number of bulk states is discrete for each value of q_{\parallel} , and is related to the number of layers in the simulation. We do not believe that this is a major limitation, essentially because all the relevant physics occurs close to E_F , while the remaining states mainly act as a polarizable background. The electrons are allowed to move and interact only in the z -direction, perpendicular to the surface, and we assume a parabolic dispersion in the parallel direction. Within this approximation, the Hamiltonian describing such system can be written as

$$\hat{H}_0 = -\frac{d^2}{dz^2} + \hat{v}_{\text{model}}. \quad (3)$$

This operator is discretized in real-space using a grid-spacing of 0.2 a.u., which is sufficiently small to allow for a proper description of the relevant electronic states.

At $t = 0$ we assume the system to be in the ground-state of the Hamiltonian (3). We then propagate this state with the new Hamiltonian

$$\hat{H}(t) = \hat{H}_0 + \hat{v}_{\text{laser}}(z, t) + \hat{\Sigma}(z), \quad (4)$$

where $\hat{v}_{\text{laser}}(z, t)$ describes a laser polarized in the z -direction that reads, in the length gauge, $\hat{v}_{\text{laser}}(z, t) = zE(t)$. The electric field is composed of a pump and a probe pulses,

$$E(t) = E_{\text{pump}}(t) \cos(\omega_{\text{pump}}t) + E_{\text{probe}}(t) \cos(\omega_{\text{probe}}t). \quad (5)$$

The functions $E_{\text{pump/probe}}(t)$ are envelope functions of the form

$$E_i(t) = E_i \cos^2 \left[\frac{\pi}{\sigma_i} (t - t_i) \right] \Theta(t - t_i + \sigma_i/2) \times \Theta(-t + t_i + \sigma_i/2), \quad (6)$$

where σ_i is the width of the pulse and t_i the center of the pulse. For the pump pulse, t_{pump} is simply $\sigma_{\text{pump}}/2$, while for the probe pulse $t_{\text{probe}} = t_D + \sigma_{\text{pump}}/2$, with t_D the delay time between the pump and probe lasers. In order to take into account the finite lifetime of the image potential states we add to the Hamiltonian (3) a time-independent self-energy operator of the form:

$$\Sigma(z) = -i \sum_{k=1}^N \Gamma_k |n_k\rangle \langle n_k|, \quad (7)$$

where $|n_i\rangle$ are the image potential states and Γ_k are the inverse experimental lifetimes of each state taken from Ref. [3]. Note that $\hat{H}(0) = \hat{H}_0$. The time-propagation is performed in real-time following the method of Ref. [11]. This propagation scheme preserves unitarity for a Hermitian Hamiltonian, and has been proven very robust and stable in diverse applications.

3. Energy-resolved spectra

In order to obtain the energy-resolved photoelectron spectra we follow the technique of Ref. [10] and divide the simulation box in two regions: one region, A, containing the slab and the region where the first image potential states lie, and another, B, defined as the complement of A (see Fig. 2). In region B the electrons are considered free outgoing particles, and are treated in momentum space. The separation between the two regions is achieved through a smooth masking function, M , defined as one in the interior of region A and zero outside. The method consists in evolving the wavepacket in the first region with the Hamiltonian (4), and mask the orbitals at each time-step. The electrons that “leave” region A are then treated as free-particles and accumulated in momentum space. In mathematical terms, the evolution is performed in the following way: we start by propagating the wave-functions in regions A and B using

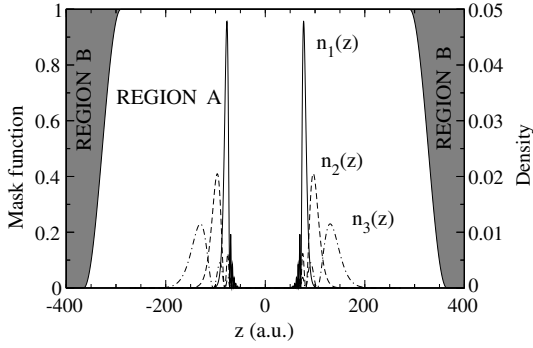


Fig. 2. Typical shape of the mask function, M , used for dividing the space in two regions (see text for details). For illustrative purposes we also plot the densities of the first three image states of Cu(100).

$$\begin{aligned} \psi_k^A(z, t + \Delta t) &= M(z) \exp(-i\hat{H}\Delta t)\psi_k^A(z, t), \\ \psi_k^B(p, t + \Delta t) &= \exp\left\{-i\frac{[p - A(t)]^2}{2}\Delta t\right\}\psi_k^B(p, t) \\ &+ \tilde{\psi}_k^A(p, t + \Delta t), \end{aligned} \quad (8)$$

where $\tilde{\psi}_k^A(p, t + \Delta t)$ is the Fourier transform of the part of the wave function ψ_k^A that left region A during the time-step Δt , i.e.,

$$\begin{aligned} \tilde{\psi}_k^A(p, t + \Delta t) &= \int dz \exp(ipz)[1 - M(z)] \\ &\times \exp(-i\hat{H}\Delta t)\psi_k^A(z, t), \end{aligned} \quad (9)$$

where p denotes the momentum. If we wait long enough after that the laser has been turned off, region B will contain those electrons that were ionized. The photoelectron spectra is then identified with

$$P(\sqrt{2mE}) = \sum_{k=1}^N |\psi_k^B(p, t \rightarrow \infty)|^2 \quad (10)$$

where N is the total number of electrons. This method can be derived from the interpretation of the Wigner transform of the one-body density matrix as a probability density [10].

In Fig. 3 we depict the energy-resolved spectra of a Cu(100) and a Cu(111) surfaces for both zero and finite pump–probe delay. For the (100) surface, the binding energies of the first image potential states are -0.57 , -0.18 and -0.08 eV (see Fig. 1) while for the (111) surface the first states are at -0.82 , -0.22 and -0.009 eV. Note that the second and third image states of the Cu(111) surface are resonances. Furthermore, the laser parameters used in these calculations were, for the (100) surface, $\hbar\omega_{\text{pump}} = 4.7$ eV, $\hbar\omega_{\text{probe}} = 1.8$ eV,

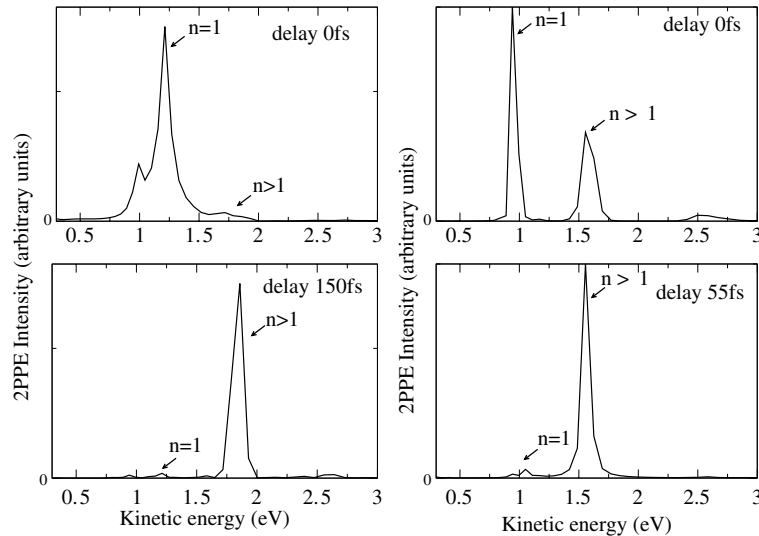


Fig. 3. Photoelectron energy-resolved spectra of a Cu(100) (left panel) and a Cu(111) (right panel) surfaces for both zero and finite pump–probe delay.

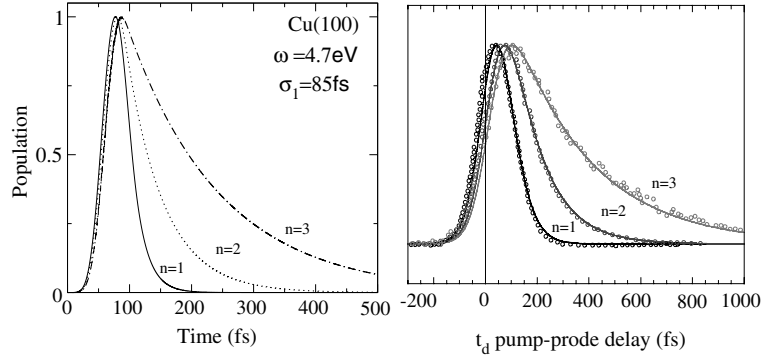


Fig. 4. Left: population of the image states $n = 1, 2$ and 3 as function of time. The values of $\Gamma_{i=1,2,3}$ appearing in Eq. (7) were taken from Ref. [3], and the maximum of each curve was normalized to one. Right: 2PPE intensity for the $n = 1, 2$ and 3 image states of Cu(100) as function of the pump-probe delay. Reproduced from Ref. [6].

$\sigma_{\text{pump}} = 95$ fs, and $\sigma_{\text{probe}} = 54$ fs, and for the (1 1 1) surface, $\hbar\omega_{\text{pump}} = 5.1$ eV, $\hbar\omega_{\text{probe}} = 1.8$ eV, $\sigma_{\text{pump}} = 87$ fs, and $\sigma_{\text{probe}} = 50$ fs. From these results we observe that the peaks corresponding to the first image potential state are obtained at the correct energy position. The signal due to the image states of higher quantum number cannot be distinguished due to the small difference in energy that cannot be resolved with our grid resolution. We also note that for zero delay, the broadening of the peak relative to the first image potential state is larger in the case of the Cu(100) surface than in the Cu(111). This is due to the fact that in the former case, the probe pulse can “pump” low lying energy electrons from the bulk into energy levels near the gap which can be then ejected from the surface by the pump pulse. As the Cu(111) surface has a different electronic structure, such situation does not occur.² Note that Cu(100) shows an intrinsic surface state resonance, while Cu(111) has a surface state below the Fermi level. In the last case, the dominant transition happens between the occupied surface state and the first image potential state. This can be rationalized in terms of the larger spacial overlap between surface and image states as compared to bulk states.

² For a schematical projection of the bulk band structure onto the (1 1 1) and (1 0 0) surfaces of Cu see, for instance, Ref. [3, p. 21].

4. Time-resolved spectra

The typical energy width of the laser pulses used in TR-2PPE varies between about 10 and 30 meV. With this energy resolution it is possible to excite separately each one of the first three image potential states of Cu(100). By following the TR-2PPE intensity in function of the pump-probe delay it is then possible to follow the evolution of the population of these states. In Fig. 4 we present calculations of the populations of the first three image states of Cu(100). The curves were obtained by propagating the system with the Hamiltonian (4). For comparison we also show the experimental data from Ref. [6]. Clearly, there is a good qualitative agreement between the theoretical and experimental curves.

In these calculations, the electron–electron interaction was taken into account by the model potential of Ref. [2]. However, the variation of this term with time was mostly neglected. Part of the time-dependence is taken indirectly into account through the self-energy operator, but one can question how reasonable this approximation really is. In order to answer to this concern, we performed simulations in which we allowed the classical part of the electron–electron interaction (i.e. the Hartree term) to change with time. This was achieved by adding to the Hamiltonian (4) a new term, $\delta v_{\text{Hartree}}(z, t)$, that corresponds to the variation of the Hartree potential due to the change of

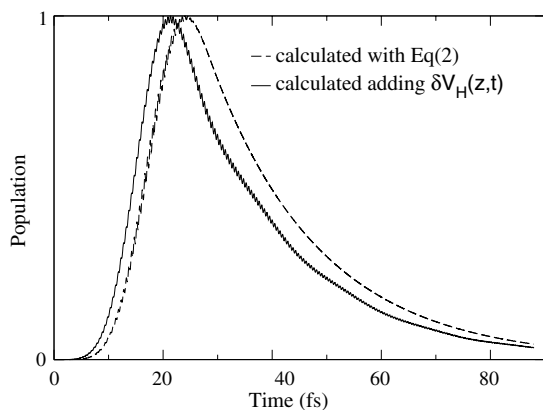


Fig. 5. Population of the first image potential state of Cu(100) calculated with and without the term of Eq. (11) for a 29 fs laser pulse of energy $\hbar\omega = 4.2$ eV. In both cases the maximum value of the population has been normalized to one. The difference in the lifetime for the two cases is 2%.

electronic density in the direction perpendicular to the surface

$$\frac{\partial^2 \delta v_{\text{Hartree}}(z, t)}{\partial z^2} = -4\pi\delta\rho(z, t), \quad (11)$$

where $\delta\rho(z, t) = \rho(z, t) - \rho(z, 0)$. Exchange and correlation effects were treated as before, i.e., through the self-energy term (7) used to simulate the lifetime of the states. The evolution of the population of the first image state with and without this term is shown in Fig. 5. We observe only a minor shift of the peak to lower times from 24 to 21.3 fs and the lifetime is reduced by around 2% when the term of Eq. (11) is included. This result validates previous studies that have neglected this effect [8].

5. Conclusions

We have performed dynamical simulations in order to calculate energy-resolved photoemission spectra of the Cu(100) and Cu(111) metal surfaces. Using the same technique we also obtained time-resolved photoemission spectra for individual excitations of the first three image potential states of Cu(100). This technique is quite general, and can be used to gain insight on the dynamics of image states with large quantum number and when

more than one eigenstate is excited coherently (the situation in quantum beat spectroscopy). Furthermore, we studied the influence of the variation of the Hartree potential during the excitation. This effects turns out to be small (around 2%).

Acknowledgements

This work was supported by the Basque Country University, DGES and European Community under the research training network NANOPHASE (HPRN-CT-2000-00167). We wish to thank H. Appel, E. K. U. Gross and P. M. Echenique, for enlightening discussions and to the high-performance computing facilities of CEPBA where most of the calculations were done.

References

- [1] P.M. Echenique, J.B. Pendry, *J. Phys. C* 11 (1978) 2065; P.M. Echenique, J.B. Pendry, *Prog. Surf. Sci.* 32 (1990) 111; P.M. Echenique, J.M. Pitarke, E.V. Chulkov, V.M. Silkin, *J. El. Spec. Rel. Phen.* 126 (2002) 163.
- [2] E.V. Chulkov, V.M. Silkin, P.M. Echenique, *Surf. Sci.* 437 (1999) 330.
- [3] P.M. Echenique, J.M. Pitarke, E.V. Chulkov, A. Rubio, *Chem. Phys.* 251 (2000) 1.
- [4] T. Fauster, Ch. Reuß, I.L. Shumay, M. Weinelt, *Chem. Phys.* 251 (2000) 111; T. Fauster, W. Steinmann, in: P. Halevi (Ed.), *Photonic Probes of Surfaces, Electromagnetic Waves: Recent Developments in Research*, 2, Elsevier, Amsterdam, 1995.
- [5] K. Giesen et al., *Phys. Rev. Lett.* 55 (1985) 300.
- [6] H. Höfer, I.L. Shumay, C. Reuß, U. Thomann, W. Wallauer, T. Fauster, *Science* 277 (1997) 1480.
- [7] T. Klamroth, P. Saalfrank, U. Höfer, *Phys. Rev. B* 64 (2001) 035420.
- [8] J. Osma, I. Sarria, E.V. Chulkov, J.M. Pitarke, P.M. Echenique, *Phys. Rev. B* 59 (1999) 10591; E.V. Chulkov, J. Osma, I. Sarria, V.M. Silkin, J.M. Pitarke, *Surf. Sci.* 433 (1999) 882; I. Sarria, J. Osma, E.V. Chulkov, J.M. Pitarke, P.M. Echenique, *Phys. Rev. B* 60 (1999) 11795; E.V. Chulkov, I. Sarria, V.M. Silkin, J.M. Pitarke, P.M. Echenique, *Phys. Rev. Lett.* 80 (1998) 4947.
- [9] J.D. McNeil, N.H. Ge, C.M. Wong, R.E. Jordan, C.B. Harris, *Phys. Rev. Lett.* 79 (1997) 4645.
- [10] D. Varsano, M.A.L. Marques, H. Appel, E.K.U. Gross, A. Rubio, to be published.
- [11] M.A.L. Marques, A. Castro, G.F. Bertsch, A. Rubio, *Comput. Phys. Commun.* 151 (2003) 60.